



Aeroelastic Analysis of an Atypical Geometry Building by Solving Fluid-structure Interaction Problem through Load Transmission Method

**Noé Díaz-Briceño¹, Jaime Moisés Horta-Rangel^{1*},
Jesús Gerardo Valdés-Vázquez², Miguel Ángel Pérez-Lara-y-Hernández¹
and Guadalupe Moisés Arroyo Contreras¹**

¹Department of Graduate Engineering, Universidad Autonoma de Queretaro, Cerro de las Campanas
s/n Querétaro, Qro. C. P. 76010, Mexico.

²Department of Civil Engineering, Universidad de Guanajuato, Ave. Juárez 77 Guanajuato, Gto.
C.P. 36000, Mexico.

Authors' contributions

This work was carried out in collaboration between all authors. All authors read and approved the final manuscript.

Article Information

DOI: 10.9734/CJAST/2018/45332

Editor(s):

(1) Dr. Jakub Kostecki, Professor, Faculty of Civil Engineering, Architecture and Environmental Engineering, University of Zielona Góra, Poland.

Reviewers:

(1) Marin Marin, Transilvania University of Brasov, Romania.

(2) Van-Dang Nguyen, KTH Royal Institute of Technology, Sweden.

Complete Peer review History: <http://www.sciencedomain.org/review-history/27256>

Original Research Article

Received 06 September 2018

Accepted 13 November 2018

Published 16 November 2018

ABSTRACT

Aims: On this work, a methodology that solves the fluid-structure interaction problem through load transmission method approach is presented. This methodology is applicable to any building's geometry, nevertheless, in order to develop a solution, it was proposed a building with a geometry not considered in design codes of structures under wind pressures. In order to compare the results of this methodology a tall building model widely studied by different authors is also analysed.

Place and Duration of Study: Graduate Engineering Department, Universidad Autonoma de Queretaro, Queretaro, Mexico. January 2017 to October 2018.

Methodology: First of all, two computational fluid mechanics models were developed in order to obtain the pressures of the wind around the two buildings proposed in a dynamic way. Later, the obtained dynamic pressures were transferred according to the load transfer method on the

*Corresponding author: E-mail: jaimhorta@prodigy.net.mx, horta@uaq.mx;

Structural Mechanical Building model through time-history analysis solved by means of a direct integration method to obtain the dynamic aeroelastic response of the structures.

Results: The dynamic aeroelastic response for both models is obtained.

Conclusion: This methodology does not present any restriction in the model's geometry and leads to analyse important aspects for the structural analysis such as state of stress of the structural elements and structure displacements, accordingly, the method is suitable for structures under wind pressures that are not considered in the codes. The results obtained through this methodology present a good approach to those obtained by means of fluid structure-interaction models.

Keywords: Aeroelastic analysis; load transfer method; fluid-structure interaction; computational fluid mechanics; dynamic analysis.

1. INTRODUCTION

The wind behaves in a dynamical way both in time and in the space, such a behaviour can only be described as random due to such complexity [1]. The different responses due to the relation between wind pressures and structures are essential in the building design, particularly in high-rise buildings [2]. The effects generated by wind pressures on structures lead to serious consequences, even tragic events depending on the presented conditions.

The dynamic response of a structure under wind loads depends mainly on these three factors [3]: direction of the wind, physics and aerodynamics properties of the structure and the combined effect of the wind and building properties. Besides, the environment surrounding the building should be considered [4]. The common practice to model wind pressures proposed by the construction design codes is simply to apply the loads in a static way through few pressure coefficients, ignoring the dynamic behaviour of the wind [2].

Nowadays, structures with particular aerodynamic problems have found a numerical solution with the development of the Computational Fluid Dynamic (CFD), which solves the Navier-Stokes equations for not compressive fluids, dealing with the solid (structure) as an obstacle in the direction of the fluid, since the solid is considered rigid, whereby, it does not present displacements due to the wind pressure. Through this technic, dynamic wind pressures on the surface of the building can be obtained, besides, wind velocities, even, the vortices around the solid can be observed. For a good understanding of the beginning of the CFD in building technology, see references [5,6,7]. At the present time, the Computational Wind Engineering (CWE) as a branch of the CFD specialised in wind problems have advanced

exponentially, nowadays, it is used by researchers and engineers all over the world [8]. Recent examples of the application of the CWE might be seen in references [4,9,10,11].

A step forward in the analysis of structures under wind pressures with particular aerodynamic characteristics was presented with the development of the Fluid-Structure Interaction (FSI) analysis. FSI is considered a multiphysic problem, since two domains are in consideration: fluid domain and solid domain. Also, the solution requires a specific condition to control the interface of the domains [12], for which a non-linear boundary condition for the fluid movement is needed, situation that complicates the problem [13]. In addition, FSI problems demand great computational capacity. FSI could be seen in a great variety of physical problems that go from engineering problems, such as high-rise buildings and long-span bridges, and biological issues as the function of the human lungs [14].

Commonly, FSI problems can be summarised as following: the fluid exerts pressure on the surface of the building, then, the pressure deforms the structure which in turn changes the dynamic of the fluid, over and over. This interaction between the domains implies that in order to model the mesh of the fluid through dynamic methods the fluid equations should adapt to those effects and to the boundary conditions.

FSI applications on buildings are shown in the work presented by Péntek et al. [15], in which based on the Commonwealth Advisory Aeronautical Council Standard (CAARC) a tall building model was tested using FSI for different types of added mass dampers using fully coupled FSI procedure. Another example of the analysis of the CAARC model using a fully coupled FSI procedure was performed by Braun and Awruch [16] whose purpose was to study the aeroelastic performance of the model. The model

was tested for different wind velocities and the results were compared to reduced scale wind tunnel test with good approximations in the results. In Horta-Rangel et al. [17] a fully coupled FSI model was proposed for an irregular medium height building model, and the obtained results were compared to reduced wind tunnel test, obtaining moderate differences between numerical model and experimental model. While Huang et al. [18] proved the simulation of a combined methodology for models suitable for relative coarse grid situations and simulation of high Reynolds number flows, with the purpose of obtaining a methodology with a great capacity for fully coupled FSI procedure for high rise buildings. In Huang et al. [18] the CAARC building model was tested, besides a full-scale Taipei high-rise model. The results for both models shown a good agreement with the experimental data. Other types of structures besides buildings have also been analysed. A 90 m steel chimney was analysed using a simplified FSI approach in Belver et al. [19]. The approach here, has consisted in the calculation of the forces in 2D fluid planes based in the CFD theory combined with the proposed structural mechanical model.

This research effort is focused in the analysis of the aeroelastic effects of an atypical geometry building by means the load transmission method, through the CFD, by applying the dynamic results obtained with CFD to a flexible model equivalent to the rigid model. This FSI approach is also known as one-way coupling. Hence, fluid domain and solid domain are not solved at the same time (two-way coupling), but in an independent way, totally ignoring the coupling of the equations. This is possible under the foundation of which the displacements on a medium-rise-building should be moderated, thus, the movement of the building do not modify the flow of the fluid significantly [15]. In order to test the capability of this methodology to approximate the results obtained through FSI method, the CAARC tall building model was tested. The results obtained on this work are compared to the results presented by Braun and Awruch [16].

2. MATERIALS AND METHODS

2.1 Numerical Model to Simulate Wind Flows

The CFD is basically a simulation based in numerical models used to predict the dynamic of the flow by solving the movement equations of

the modeled fluid as a set of points. The fluid flow is idealised through governing equations obtained from momentum, mass and energy balances over the spatial domain. In CWE wind flow can be summarised in the following points [16]:

- Wind streams are proposed within the incompressible flow range.
- Wind streams are proposed within the turbulent flow range.
- The wind is idealised to be in an isothermal process (temperature is always constant).
- In the fluid field the gravity force is neglected.
- The air is idealised as a Newtonian fluid.

The governing equations are the incompressibility condition (1), and the Navier-Stokes equations (2), [20]:

$$\operatorname{div} v = 0, \quad (1)$$

$$\rho_0 [v' + (\operatorname{grad} v)v] = \mu \Delta v - \operatorname{grad} \pi + b, \quad (2)$$

Where v , π , ρ_0 , μ and b represent the velocity, the pressure, the density, the viscosity and the body forces, respectively. While grad is the gradient operator, Δ is the Laplacian operator and v' denote the velocity derivative in time.

2.2 Numerical Model FOR Structural Dynamics

A numerical model to simulate the dynamic of a building present the following characteristics [16]:

- The material used to model the structure is linear elastic.
- There is not heat exchange during the process of energy equilibrium (isothermal process).
- Large displacements may occur in the structure; thus, a geometrical nonlinear approach may be necessary in order to describe the mechanical equilibrium correctly.

The momentum equations, the mass conservation principle and the material constitutive law, are the governing equations for the structural motion analysis [16]. The equation of movement for a multiple degrees of freedom system is given by equation (3), [21]. Equation (3) is basically obtained from the governing equations previously mentioned, considering a

Lagrangian formulation that is expressed in the finite element context [16].

$$[M]\{\ddot{u}\} + [C]\{\dot{u}\} + [K]\{u\} = P(t). \quad (3)$$

Where $[M]$, $[C]$ y $[K]$ are the mass matrix, damping matrix and stiffness matrix respectively. While $\{u\}$ is the displacement vector, $\{\dot{u}\}$ the velocity vector, $\{\ddot{u}\}$ the acceleration vector and $P(t)$ are the external forces in time.

2.3 Direct Integration Methods

Direct integration methods are used to solve initial value problems through step-by-step integration in time. Therefore, the displacements, u_0 and the velocities \dot{u}_0 are assumed as known in a given time, $t = 0$. The period of time in which the result is sought is divided in time increments, and the direct integration method is solved approaching the solution for every time step. Examples of this kind of analysis are reviewed in this work. Detailed information about the reviewed method is presented in Horta-Rangel et al. [17].

2.3.1 Newmark method

In 1950 N. M. Newmark developed a group of time-step methods based on the following equations:

$$\dot{u}_{n+1} = \dot{u} + \Delta t[\gamma\ddot{u}_{n+1} + (1 - \gamma)\ddot{u}_n], \quad (4)$$

$$u_{n+1} = u_n + \Delta t\dot{u}_n + \frac{\Delta t^2}{2}[2\beta\ddot{u}_{n+1} + (1 - 2\beta)\ddot{u}_n], \quad (5)$$

Where γ and β defined the variation of acceleration during a time step and determined the characteristics of stability and stability of the method. Usually, $\gamma = \frac{1}{2}$, while $\frac{1}{6} \leq \beta \leq \frac{1}{4}$. Equations (4) and (5) combined with equation (3), at the end of the time step is the basis to compute u_{i+1} , \dot{u}_i y \ddot{u}_{i+1} in time $i + 1$ from u_i , \dot{u}_i and \ddot{u}_i known in time i .

2.3.2 Hilbert-Hughes-Taylor

This is an implicit method that can handle numerical damping, without degrading the order of accuracy. This method is convenient because introducing Rayleigh proportional damping in the Newmark method mostly damps just the middle modes, and barely affects the higher and lower modes. These limitations can be overcome by introducing algorithmic damping in the Newmark

method by assigning γ with a value larger than 0.5. The problem about this solution is a reduction in the accuracy. In the Hilbert-Hughes-Taylor method the approximation of the Newmark method, shown in the equation (4) and equation (5), are used.

2.3.3 Wilson method

Information about this method was extracted from Meruane [22]. In the Wilson method a linear variation of the acceleration is assumed between a time step t and $t + \theta\Delta t$, where $\theta \geq 1$. Assuming $\theta = 1$, the method is reduced to a linear acceleration scheme. But, in order to ensure unconditional stability is necessary to use $\theta \geq 1.37$, usually $\theta = 1.4$.

Assuming τ is the time increment, where $0 \leq \tau \leq \theta\Delta t$ then:

$$\ddot{u}(t + \tau) = \ddot{u}(t) + \frac{\tau}{\theta\Delta t}(\ddot{u}(t + \theta\Delta t) - \ddot{u}(t)). \quad (6)$$

From equation (6), the solution for displacements, velocity and acceleration can be obtained.

$$u(t + \theta\Delta t) = u(t) + \theta\Delta t\dot{u}(t) + \frac{\theta^2\Delta t^2}{6}(\ddot{u}(t + \theta\Delta t) + 2\ddot{u}(t)), \quad (7)$$

$$\dot{u}(t + \theta\Delta t) = \frac{3}{\theta\Delta t}(u(t + \theta\Delta t) - u(t)) - 2\dot{u}(t) - \frac{\theta\Delta t}{2}\ddot{u}(t), \quad (8)$$

$$\ddot{u}(t + \theta\Delta t) = \frac{6}{\theta^2\Delta t^2}(u(t + \theta\Delta t) - u(t)) - \frac{6}{\theta\Delta t}\dot{u}(t) - 2\ddot{u}(t), \quad (9)$$

2.4 Methodology

A fluid-structure analysis approach is presented in this work. Two models are analysed, one is the tall building CAARC model, (Commonwealth Advisory Aeronautical Council standard), and the other is a fictitious building whose geometry is not very common, in such a way that it is not considered in the building design codes under wind pressures. The principal reason to test the first model is to have a comparison point (since it has been widely tested) to analyse the competence of this methodology; for this model, only an elastoplastic analysis was done. In the other hand, the atypical geometry building is tested to prove that this methodology can overcome the deficiencies presented in the current building design codes under wind pressures both in geometry and in dynamic performance: for this model, an aeroelastic analysis were executed.

2.4.1 Fluid flow solution

In order to perform the proposed analysis, first of all, a CFD analysis should be performed. In order to complete that task, the “Autodesk Robot Structural Analysis Professional Software” were used to analyse the dynamic pressures on the surfaces of the models. For the aerodynamic analysis, “Autodesk Flow Design” were used. Both programs use the numerical technique for the flow analysis known as large eddy simulation (LES) type approach using a finite volume method (FVM) and a transient, incompressible fluid flow solver (flow design solver). For a brief explanation of the programs used to perform the fluid analysis refer to Autodesk [23,24]. The flow mesh is an important aspect to obtain the correct results in a CFD analysis. Even with the great advance in the CFD technology, the correct size of the mesh is unknown, most of the researches propose the mesh based on their personal experiences [25]. For practical guidance for mesh size see Zhang and Yu [26], Stephen [27]. In the chosen program for the fluid analysis, the mesh size is done automatically by the program. Once the model is running correctly, the pressures on the surfaces should be registered for every specific surface area. Every section of the surface’s model was partitioned and carefully named.

2.4.2 Structural dynamic solution

With the dynamic pressure correctly registered and organised, the elastic model was prepared in the structural analysis and design program “Sap 2000” for both proposed models. See Dørheim [28] for detail information about direct integration through SAP 2000. Every node of the structural model is named, and the registered pressures for that specific area in which the load is located was assigned. For the variation in time of the loads, and specific function for every node that defines the change in amount of pressure were assigned, in such a way that all the functions work at the same time varying the loads and generating the solution for specific time steps. Sap 2000 uses Newmark method to perform the non-linear analysis with coefficients $\gamma = \frac{1}{2}$ and $\beta = \frac{1}{6}$. From this analysis, the dynamic displacements of the structure and the dynamic state of stresses of the elements that compose the structure are obtained.

2.5 Properties of the CAARC Model

The CAARC model was proposed for the first time in 1970 [16]. The original purpose of the CAARC building model was to run experiments in a reduced scale wind tunnel. With the pass of the years, the CAARC model became a model used to calibrate wind tunnels all around the world. Two CAARC models were proposed, one is very simple as a benchmark model, it is called ‘Building B’, and there is a more complex model named ‘Building A’ [16]. For the purposes of this investigation, only the Building B is tested. The dimension of the CAARC model are presented below:

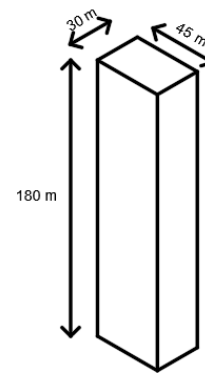


Fig. 1. Dimensions of the CAARC model

As shown in Fig. 1, the building is 180 m high, the cross section is rectangular, with horizontal section of 45 m by 30 m. In regard to the structural dynamic part, the mass and stiffness properties were proposed constant in the whole structure. The density is taken as 160 kg/m^3 with an elasticity modulus of $2.861e8 \text{ N/m}^2$, the first eigenfrequency according to the dynamic properties is equal to 0.2 Hz (5 s) [16]. The CAARC building can be modeled simply as a cantilever beam. For this work, the CAARC model was modeled with block solid elements with the geometry presented in Fig. 2, and the mechanical properties previously described. The model is fixed on its supports.

For the finite volume mesh, it is important to remark that as it was explained before, the mesh is generated by the program itself, but, the size of the “virtual wind tunnel” (space occupied by the mesh of the fluid) can be modified. The dimensions for the virtual and its position regarding to the CAARC model are presented in Fig. 3.

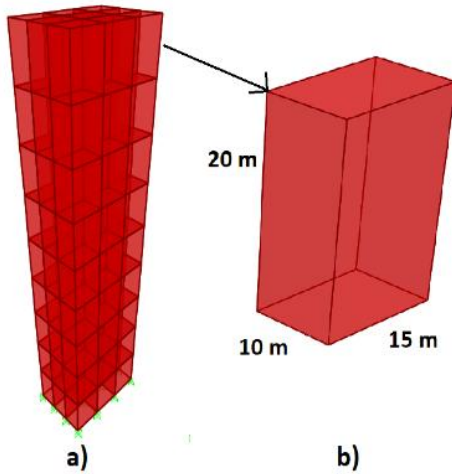


Fig. 2. a) CAARC model in Sap 2000 b) geometry of the solid elements that conform the model

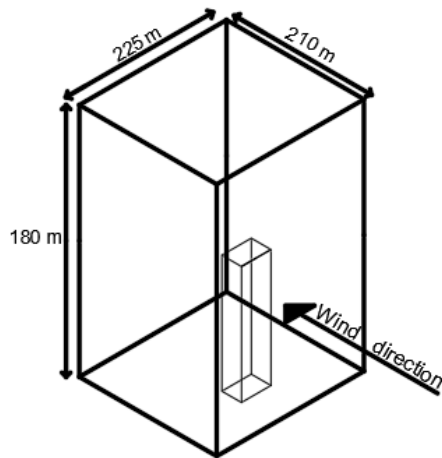


Fig. 3. Virtual wind tunnel of the CAARC model

As might be seen in the Fig. 3 the wind direction is also indicated. The dimensions of the virtual wind tunnel correspond to the following parameters:

- Width: five times the width of the building.
- Long: two times in the front of the building and four times behind the building (considering de wind direction).
- Height: two time the height of the building.

The wind properties that were used for the CAARC model test are same utilised in [16], so the result may be compared to the results of this authors' article; even though, the authors

performed several analyses for different wind velocities, only the analysis with a reduction factor of the wind velocity of 4 (36 m/s on the top of the building) were performed in this research work.

On the ground, the wind velocity slows down due to the obstacles and the ground roughness. Very above ground in layers of undisturbed wind air (around 5 km.), the wind is no longer influenced by the ground conditions. Between these two layers, the wind velocity changes with height. This effect can be approximate with a logarithmic profile.

The wind velocity profile for this analysis is presented in Fig. 4.

As might be seen in Fig. 4, the height of the virtual wind tunnel is the height of the wind velocity profile. It is important to note that the great height of the CAARC building could present great displacements, so, it might not be appropriated for a one-way coupling fluid-structure interaction model as the presented in this work, that is the reason why the wind velocity is moderate, in order to present small displacements that could not modify the dynamic of the wind importantly. The air density (ρ) is 1.20 kg/m^3 and the kinematic viscosity (ν) for air is $15.11 \cdot 10^{-6} \text{ m}^2/\text{s}$. These parameters are considered constant over the height of the building. The Reynolds number is computed on the free stream velocity at reference height (36 m/s) with the use of the following equation:

$$Re = \frac{v_{ref} \cdot B}{\nu} = 1.07e8. \quad (10)$$

Where R_e is the Reynolds number, B is the width of the building model, and v_{ref} denotes the reference velocity.

2.6 Atypical Geometry Building

The proposed building for this research work is composed by steel frames with 15 stories (4 meters between every story). The frames support slabs of 0.12 m of thickness as floor system. The building's geometry is proposed in disagreement with the geometries regulated by design codes for buildings under wind loads in such a way that an exhaustive wind pressure analysis was necessary (Fig. 5). The building is all covered in glass on the facades, so the fluid (wind) cannot enter into the building.

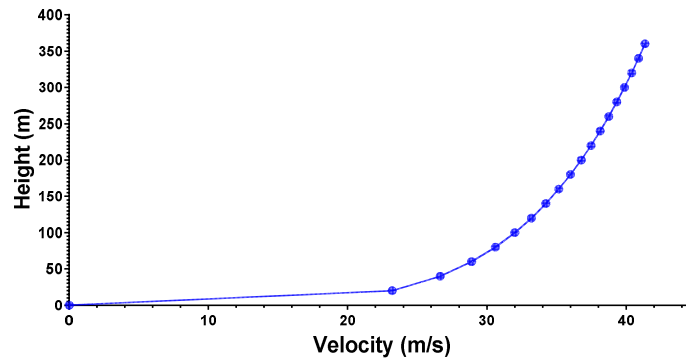


Fig. 4. Wind velocity profile for the CAARC model

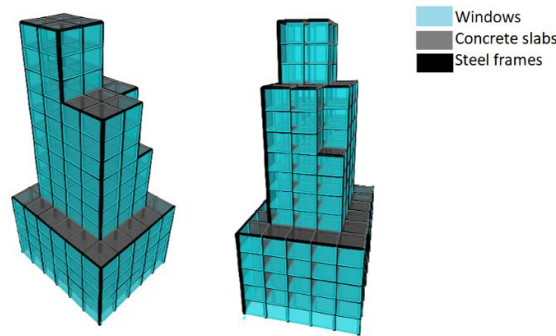


Fig. 5. Finite element model for the atypical geometry building

Table 1. Building geometry regarding the height

Floors	Height (m)	Length (m)	Width (m)	Area (m ²)
First to fifth	0-20	25	30	750
Sixth to ninth	20-36	15	20	300
Tenth to twelfth	36-48	15	20	285
Thirteenth to fourteenth	48-60	10	10	100

The dimensions of the stories vary with the height of the building as presented in Table 1.

The building is relatively tall and slender, since structures with this characteristic are particularly sensible to the effects generated by vortices around. The model is fixed on its supports.

In order to model the structure as a flexible model, two types of finite elements were used:

- Beam elements with 12 degrees of freedom (six degrees of freedom per node) used to model the frames.
- Plate elements with 24 degrees of freedom (six degrees per node) used to model the slabs and the wind on the facades.

For the structural model a static analysis was developed to assign proper structural sections to the beam and columns that form the frames in order to obtain moderate displacements, since large displacements might modify the dynamic of the fluid, situation not considered in this research effort. For the beam sections, the commercial structural profile W12x22. For the column sections, the structural profile proposed is HSS 16x16x1/2. Both profiles are made of structural steel grade 50, therefore: yield stress is equal to 344,703,747.5 n/m², and modulus of elasticity equal to 199,947,973,176.35 n/m², and mass per unit volume of 7,849 kg/m³. The concrete used in the slabs has a modulus of elasticity equal to 24,855,542,824 n/m², compressive strength equal to 27,458,620 n/m² and mass per unit volume of 2,400 kg/m³.

The wind characteristics were selected to be as critical as possible for the structure. The wind characteristics of the Mexican port city “Puerto Vallarta” were chosen due to the high regional velocity presented in the area of 160 km/h, according to the Mexican code [29] and its low location in relation to the sea level (15 m). Also, the surface roughness is negligible (terrain category of 1), making this location critical in terms of building design under wind pressures.

The Mexican code proposed the following equation (6), in order to obtain the basic wind velocity of design:

$$V_D = F_T F_{rz} V_R. \quad (11)$$

Where F_T depends on the local topography, F_{rz} depends on the section area of the structure and V_R depends on the wind velocities records for the selected region. The design velocity (66 m/s) was used in order to simulate the wind tunnel. The following equation was used to calculate the wind velocity profile:

$$V_2 = V_1 \frac{\ln(\frac{h_2}{z_0})}{\ln(\frac{h_1}{z_0})}. \quad (12)$$

Where V_1 is the wind velocity at the ground (velocity of reference), V_2 is the velocity at height h_2 and z_0 is the roughness factor (0.6 according to the terrain category). In the Fig. 6, the wind velocity profile is presented.

The Reynolds number for this model were computed in the same way it was calculated for the CAARC model. $Re = 2.18e8$ for the atypical geometry building.

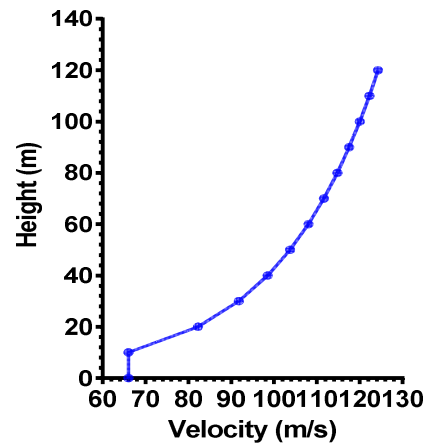


Fig. 6. Wind velocity profile for the atypical geometry building

The dimensions of the virtual wind tunnel used for this model follow up the parameters presented in the section 2.4, thus, the virtual wind tunnel present the following dimensions: width: 125 m, long: 210 m and height: 120 m.

2.6 Obtaining Pressures

The pressures are obtained through the CFD analysis on the models as colored contours on the facades that represent the mean pressure on a specific area and time. For the CAARC model, 100 s of analysis were performed, while, for the atypical geometry building, five seconds of analysis were performed (Fig. 7).

As might be seen in Fig. 7, every color contour represents a pressure in kg/m². As time passes, a specific area experiments variation in the color contours.

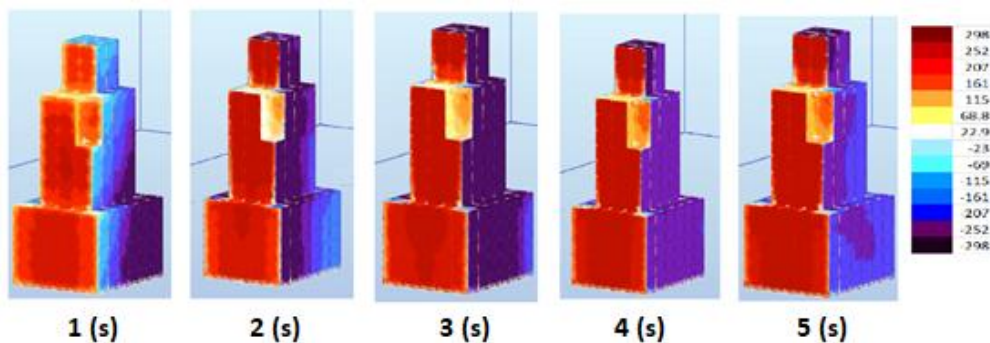


Fig. 7. Pressures on the structure in the 5 seconds considered

Note that a figure for the wind pressure analysis for the CAARC model is not presented, it is because the analysis is so long that a lot of pictures would be necessary, therefore, the atypical geometry building was more representative.

For the purpose of the registration of these pressures in order to apply them to the flexible models, an exhaustive database of the pressures was accomplished by assigning it to the node number that correspond to the area.

The nodes which pressures varies in time in the same manner were grouped in the same set of dynamic analysis. Several sets were proposed in order to capture the dynamic pressure of the CFD analysis and replicate them on the flexible model in form of nodal forces.

3. RESULTS AND DISCUSSION

In this section, the aeroelastic response for the both proposed models are presented.

3.1 Aeroelastic Response of the CAARC Model

In the following figure (Fig. 8) the displacements in the top of the CAARC model building for the two principal directions are presented.

Note that results go from $t = 25 s$ to $t = 100 s$, it is because the first 24 s are an initial ramp-up used to gradually increase the inlet velocity. This permit avoiding any shock effects early in the simulation, which could present a negative effect in the analysis. The results obtained are in good

concordance with the results presented in Braun and Awruch [16], since the form of the graph is very similar. Although, the amplitude obtained in this work is slightly smaller than the amplitude presented in the literature in the longitudinal axis. The maximum displacement presented in Braun and Awruch [16] fluctuates between 40 and 42 cm in comparison with the obtain maximum amplitude between 28 and 26 cm. The authors consider that the difference is not relevant if it is considered that the building is 180 m height, and also, the approach proposed by Braun and Awruch [16] is fully-coupled model. Regarding to the transversal response, the displacements present good concordance.

3.2 Aeroelastic Response of the Atypical Building Model

The displacements on the top of the structure are presented in the following figures (Fig. 9 and Fig. 10).

For a better understanding of the last two figures, in the next figure (Fig. 11) the displacements are plotted.

It might be seen from the past figures that the longitudinal displacements are the largest as expected, and the displacements behave in a back and forth manner. The displacements presented in the transversal axis are much smaller. A remarkable aspect about the displacements in the transversal axis is that the movement in the building cross the neutral axis in a back and forth movement, this means, that the aeroelastic phenomenon known as “vortex shedding” is occurring. This phenomenon is

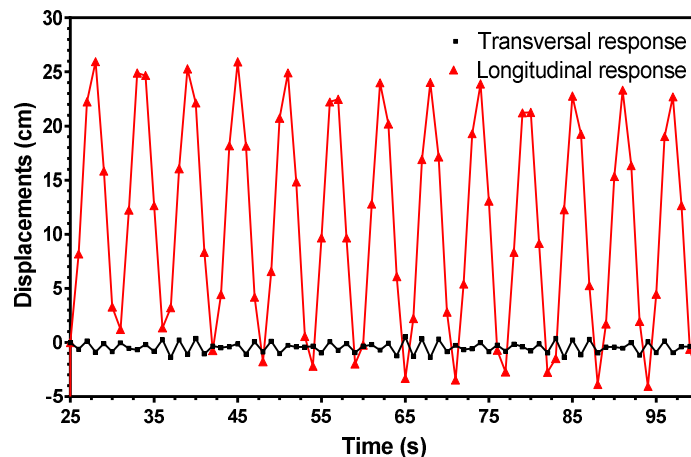


Fig. 8. Displacements in CAARC model due to dynamic wind pressures

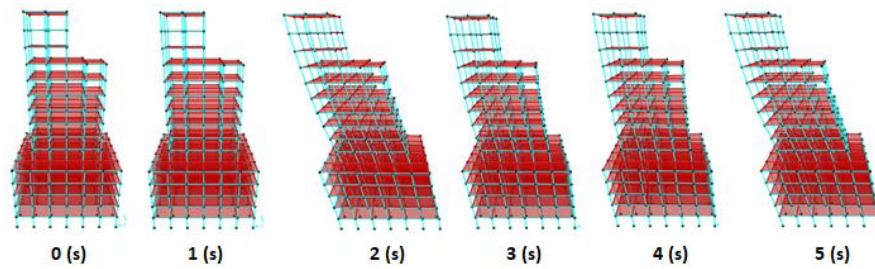


Fig. 9. Displacements in longitudinal axis in the model in time

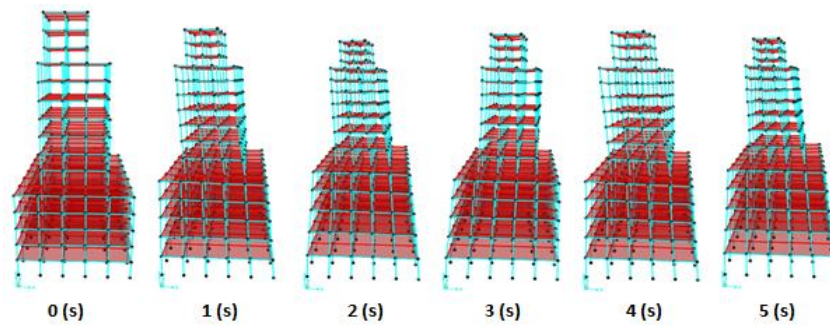


Fig. 10. Displacements in transversal axis in the model in time

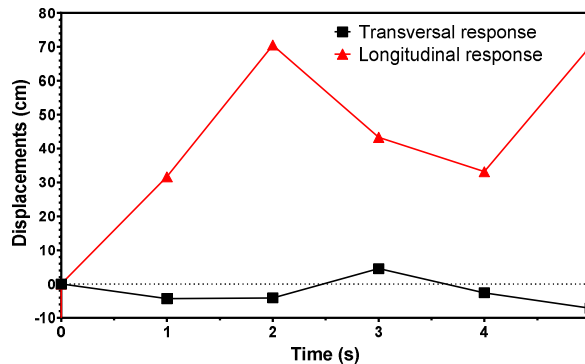


Fig. 11. Displacements in the atypical geometry model due to the dynamic wind pressures

usual in tall and slender structures under wind pressures, and commonly present vibration effects in the transversal axis that can present uncomfortable conditions for the occupants of the building.

The state of stress of the elements that conform the atypical building in time are presented in Fig. 12.

Any state of stress (axial forces, shear forces, torsional forces and bending moments) in time could be display in the model, but, only the bending moment in the vertical axis ("z") is presented in Fig. 12 just for demonstration purposes.

In order to observe the variation of the state of stress due to dynamic wind pressures, a column in the base of the building were chosen to observe its bending moment in time, because columns are the structural elements that absorb most of the wind loading as bending moments, but, any other kind of element could have been chosen. In Fig. 13, the variation of the bending moment can be seen for the 5 s of analysis. It could be seen that the bending moment can vary a lot from one second to the following second, and, as seen in the displacements, can even go back to a former bending moment value.

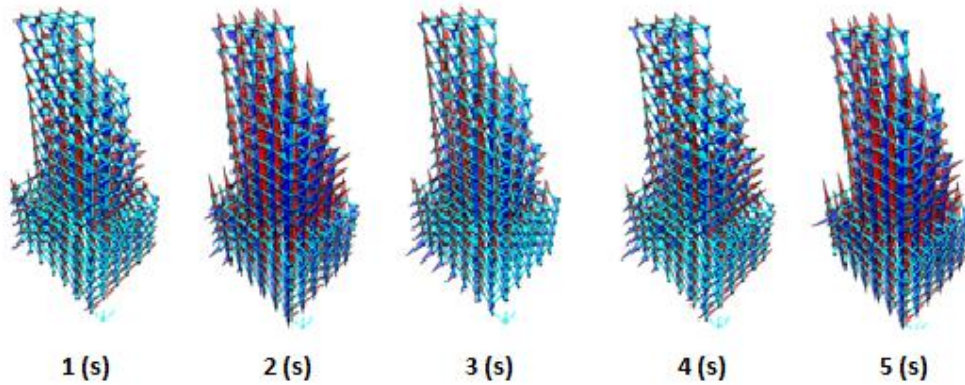


Fig. 12. Bending moment in “z” axis in time on the whole atypical geometry building model

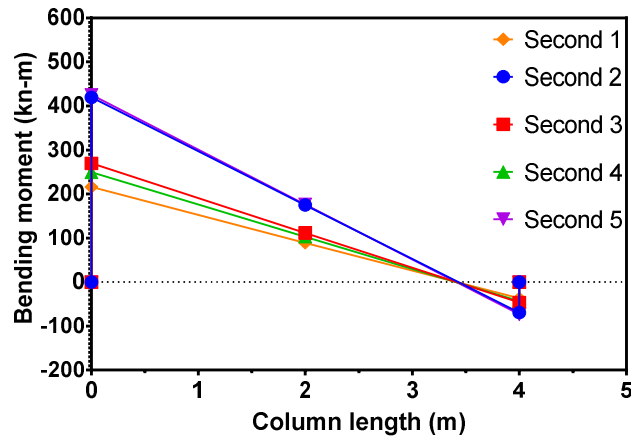


Fig. 13. Variation of the bending moments of one column on the base of the building in time

4. CONCLUSION

The proposed methodology in this work has demonstrated its accuracy even for a tall building with slightly difference in the results compared with the results shown in the literature by using full coupled FSI model. This methodology presents no restrictions in the geometry of the model, since a very irregular model have been presented, and the results demonstrated to be the expected according to the proposed wind properties. Also, all the necessary structural aspects for an optimal structural design can be analysed through this methodology (state of stresses of the structural elements and displacements) in a dynamic way. Therefore, this methodology covers all the aspects to simulate real conditions, situation not totally cover by the official codes for structural design under wind loads. The methodology does not demand a great computational power, instead, the aeroelastic analysis does not require long

computer time to finish once the pressures have been properly assigned since it finishes in few minutes even for long time analysis like the presented for the CAARC model. Considering that some reviewed methodologies can take hours or even more than one day, this methodology is efficient in time. For further studies, the authors proposed to test the atypical building model in a reduced scale wind tunnel in order to corroborate the obtained data.

COMPETING INTERESTS

Authors have declared that no competing interests exist.

REFERENCES

1. Boggs D, Dragovich J. The Nature of wind loads and dynamic response. ACI. SP. 2006;240:15–44.

2. Kopp GA, Morrison MJ, Henderson DJ. Full-scale testing of low-rise, residential buildings with realistic wind loads. *J. Wind Eng. Ind. Aerodyn.* 2012;104–106:25–39.
3. Sentile C, Noa M, Fernández V, Domínguez MFJ. Fundamento estadístico del efecto aleatorio del viento para el cálculo de estructuras delgadas. *Ing. Mec.* 2006;9:13–19.
4. Meng FQ, He BJ, Zhu J, Zhao DX, Darko A, Zhao ZQ. Sensitivity analysis of wind pressure coefficients on CAARC standard tall buildings in CFD simulations. *J. Build. Eng.* 2018;16:146–158.
DOI: 10.1016/j.job.2018.01.004
5. Summers DM, Hanson T, Wilson C. Validation of a computer simulation of wind flow over a building model. 1986;21:97–111.
6. Murakami S. Numerical simulation of turbulent flowfield around cubic model current status and applications of k- ϕ Model and Les. *J. Wind Eng. Ind. Aerodyn.* 1990;33:139–152.
7. Hunter LJ, Wales NS. An investigation of three-dimensional characteristics of low regimes within the urban canyon. *Atmos. Environ.* 1992;26:425–432.
8. Blocken B. 50 years of computational Wind engineering : Past, present and future. *Jnl. Wind Eng. Ind. Aerodyn.* 2014;129:69–102.
DOI:10.1016/j.jweia.2014.03.008
9. Hubova O, Macak M, Konecna L, Ciglan G. External pressure coefficients on the atypical high-rise building - computing simulation and measurements in wind tunnel. *Procedia Eng.* 2017;190:488–495.
DOI:10.1016/j.proeng.2017.05.368
10. Lee DSH. Impacts of surrounding building layers in CFD wind simulations. *Energy Procedia.* 2017;122:50–55.
DOI:10.1016/j.egypro.2017.07.313
11. Valdés-Vázquez JG, Villalpando-Granados GI, Hernandez-Martinez A. Ingeniería eólica en monumentos del bicentenario - Análisis por elementos finitos. *Soc. Mex. Ing. Estructural.* 2012;52:1–12. Spanish.
12. Namkoong K, Choi HG, Yoo JY. Computation of dynamic fluid-structure interaction in two-dimensional laminar flows using combined formulation. *J. Fluids Struct.* 2005;20:51–69.
DOI:10.1016/j.jfluidstructs.2004.06.008
13. Valdés-Vázquez J. Nonlinear analysis of orthotropic membrane and shell structures including fluid-structure interaction. *Universitat Politècnica de Catalunya*; 2007.
14. Förster C. Robust methods for fluid-structure interaction with stabilised finite elements. *University of Stuttgart*; 2007.
15. Péntek M, Winterstein A, Vogl M, Kupás P, Bletzinger KU, Wüchner R. A multiply-partitioned methodology for fully-coupled computational wind-structure interaction simulation considering the inclusion of arbitrary added mass dampers. *J. Wind Eng. Ind. Aerodyn.* 2018;177:117–135.
DOI:10.1016/j.jweia.2018.03.010
16. Braun AL, Awruch AM. Aerodynamic and aeroelastic analyses on the CAARC standard tall building model using numerical simulation. *Comput. Struct.* 2009;87:564–581.
DOI:10.1016/j.compstruc.2009.02.002
17. Horta-Rangel JM, Lara-Lpoez JP, Váldez-Vázquez JG, Arreola-Sinfuentes I. Fluid-structure interaction and aeroelastic balance on the analysis of a tall building with irregular geometry. *Br. J. Appl. Sci. Technol.* 2016;13:1–14.
DOI:10.9734/BJAST/2016/22578
18. Huang S, Li R, Li Q. Numerical simulation on fluid-structure interaction of wind around super-tall building at high reynolds number conditions. *Struct. Eng. Mech.* 2013;46:197–212.
DOI:10.12989/sem.2013.46.2.197
19. Belder, A. V., A. L. Ibán, and C. E. Lavín Martín. 2012. Coupling between structural and fluid dynamic problems applied to vortex shedding in a 90m steel chimney. *J. Wind Eng. Ind. Aerodyn.* 100:30–37.
DOI:10.1016/j.jweia.2011.10.007.
20. Gurtin EM. An introduction to continuum mechanics. First Edit. Academic Press, Inc., Pittsburg, Pennsylvania; 1981.
21. Chopra AK. *Dinámica de estructuras.* Cuarta edi. Pearson, Naucalpan de Jauarez, Estado de México. Spanish; 2014.
22. Meruane V. *Dinámica Estructural.* 130. Spanish; 2006.
23. Autodesk. Autodesk Robot Structural Analysis Professional wind simulator validation brief; 2015.
Available:<https://bimandbeam.typepad.com/files/robot-structural-analysis-professional-wind-simulator-validation-brief.pdf?fbclid=IwAR0ampV8aOs2xhNYqCnnQ06WXOc4Hb6YjAnkb43FvsFZfyCISjor0oePS5o>

24. Autodesk. Flow Design Preliminary Validation Brief. 2013;11. Available:http://d2cw6w4qme40ds.cloudfront.net/uploads/reports/files/000/000/014/original/Flow_Design_Wind_Tunnel_Validation_Brief.pdf?1402064063
25. Yu F, Zhang H, Li Y, Xiao J, Class A, Jordan T. Voxelization-based high-efficiency mesh generation method for parallel CFD code GASFLOW-MPI. Ann. Nucl. Energy. 2018;117:277–289. DOI:10.1016/j.anucene.2018.03.045.
26. Zhang HR, Yu Y. A guidance to grid size design for CFD numerical simulation of hypersonic flows. 2013;67:178–187. DOI:10.1016/j.proeng.2013.12.017
27. Stephen AJ. A structured-grid quality measure for simulated hypersonic flows. In: 42nd AIAA Aerospace Sciences Meeting and EXHIBIT. NASA Langley Research Center Hampton, Reno, Nevada. 2004;23681–2199.
28. Dørheim H. Methods for earthquake analysis. 2012;92.
29. Comisión Federal de Electricidad. Diseño por viento. In: Manual de Diseño de Obras Civiles. Comisión Federal de Electricidad, México, D.F. Spanish. 2008;360.

© 2018 Díaz-Briceño et al.; This is an Open Access article distributed under the terms of the Creative Commons Attribution License (<http://creativecommons.org/licenses/by/4.0>), which permits unrestricted use, distribution, and reproduction in any medium, provided the original work is properly cited.

Peer-review history:
The peer review history for this paper can be accessed here:
<http://www.sciencedomain.org/review-history/27256>